CrystEngComm

PAPER

Supramolecular architectures of conformationally controlled 1,3-phenyl-dioxalamic molecular clefts through hydrogen bonding and steric restraints†

Juan Saulo González-González,[a] Francisco Javier Martínez-Martínez,[a] Ana Lilia Peraza Campos,[a] Maria de Jesus Rosales-Hoz,[b] Efrén V. García-Báez[c] and Itzia I. Padilla-Martínez[*c]

In this contribution the supramolecular architecture of a series of six 1,3-phenyl-dioxalamic molecular clefts is described. The conformation was controlled by the use of Me and OMe group substitution in the phenyl spacer. The structural and conformational study was carried out by X-ray diffraction analysis, DFT calculations at PBEPBE 6-31+G (3df, 3pd) theory level and variable temperature ^{1}H NMR in solution. The C2-Me group exerts a dual influence on the conformation adopting the *endo*(*sc*) or *exo*(*ac*) conformations in the oxalamic arms, meanwhile the C2-OMe group leads to the adoption of the *exo*(*ap*) conformation. DFT study results showed that the *exo*(*ap*)–*exo*(*ap*) conformation is more stable than the other conformations due to the conjugation that stabilizes the molecule and minimizes the conformational energy. Supramolecular arrays in oxalamate/oxalamide derivatives of 1,3-diaminobenzene, 2-methyl-benzene-1,3-diamine and 2,4,6-trimethyl-benzene-1,3-diamine are directed by self-complementary N–H···O hydrogen bonding interactions, whose organization in the crystal depends on the twist of the oxalamic arms, meanwhile in oxalamate/oxalamide derivatives of 5-*tert*-butyl-2,6-diamineanisol with an *exo*(*ap*)–*exo*(*ap*) conformation, the supramolecular arrays are directed by π-stacking, dipolar carbonyl–carbonyl interactions and C–H···O soft contacts. $N^1, N^{1'}$-(1,3-(2,4,6-Trimethyl)-phenyl)-bis-(N^2-(2-(2-hydroxyethoxy)ethyl)oxalamide) adopts the form of a supramolecular *meso*-helix, which is the first example of helical 1,3-phenyl-dioxalamide.

1. Introduction

Non-covalent interactions are recognized to be involved in crystal engineering and molecular recognition.[1] They have been increasingly used as a powerful tool for construction of many supramolecular architectures, devices and nanostructured materials.[2] Among them, hydrogen bonding is particularly important from the biological point of view, because of its participation in several biological processes such as: the stabilization of the double helix of DNA,[3] enzyme–substrate interactions,[4] recognition among proteins[5] and drug–acceptor interactions.[6] Hydrogen bonding is the most important element in the design of self-assembled organic molecules, sometimes with the participation of other intermolecular forces.[7] Inter- and intra-molecular hydrogen bonding has been extensively used in the production of complex organized systems due to the reversibility, specificity, directionality and cooperativity of such interactions.

Oxalamates are composed of an amide and an ester group directly connected to each other. Thus the functionalities N–H, C=O and O–R allow them to form one dimensional (1-D) networks through intermolecular hydrogen bonding,[8] but they also can form two (2-D) and three dimensional (3-D) networks whose architecture in the solid state will depend on the side-arm substituent.

Oxalamides, which are mono-substituted diamides of oxalic acid, represent construction units with high in-plane hydrogen bonding potential; they are self-complementary and capable of unidirectional hydrogen bonding. In many cases, their self-assembly produces robust one-dimensional hydrogen-bonded chains, although, depending on the substitution and presence of additional hydrogen bonding units, a variety of more complex structures might be observed. The NH and amide carbonyl are usually in a *trans* disposition as also are amide and ester carbonyls or both carbonyl amides, in oxalamate and oxalamide, respectively, thus the most common conformation is *trans–anti* (*t,a*) in oxalamates and *trans–anti–trans* (*t,a,t*) in oxalamides.[9]

[a]*Facultad de Ciencias Químicas, Universidad de Colima, Km. 9 Carretera Colima-Coquimatlán, C.P. 28400 Coquimatlán, Colima, Mexico*
[b]*Departamento de Química, CINVESTAV-IPN, Av. Instituto Politécnico Nacional 2508, Col. San Pedro Zacatenco, Apartado postal: 14-740, 07000, C.P. 07360 México, D.F., Mexico*
[c]*Departamento de Ciencias Básicas, Unidad Profesional Interdisciplinaria de Biotecnología del Instituto Politécnico Nacional, Av. Acueducto s/n Barrio la Laguna Ticomán, 07340 México, D. F., Mexico*

Oxalamate **Oxalamide**

(t,a) *(t,a,t)*

1,3-Phenyl-dioxalamates and 1,3-phenyl-dioxalamides are good candidates to be used in molecular recognition processes, because of the cavity formed in between the two side arms with a bent conformation and the open possibility of π-stacking between the phenyl spacer. The relative disposition of both arms in relation to the 2-substituted phenyl spacer and among them gives rise to several conformations.

In this contribution the molecular and supramolecular structure of 1,3-phenyl-dioxalamate **1** is revisited, and those corresponding to three 2-substituted 1,3-phenyl-dioxalamates **2–4** are reported. This series of compounds was synthesized starting from 1,3-diaminobenzene C-2 substituted with Me or OMe groups. The presence of these groups bisecting the central phenyl ring was used to tilt the oxalyl side arms out of the plane and thus favor intermolecular hydrogen bonding. In order to test the utility of the hydroxyl group to increase the self-assembling capabilities of the oxalamide moiety into predictable structural patterns, oxalamides with side-arm substituents derived from ethanolamine **5–7** were prepared. Furthermore, the molecular and supramolecular 1,3-phenyl-dioxalamides **5–7** are also analyzed and compared with their parent dioxalamates **2–4**. To the best of our knowledge there are recent reports on the topological control[10a] of their dimensionality in the solid state, but there are no reports about the use of steric effects to control the conformation and so the hydrogen bond directed self-assembly in the solid state of these molecules. Results were supported by DFT calculations and ^{1}H NMR measurements.

1 $R_1 = R_2 = R_3 = H$
2 $R_1 = CH_3, R_2 = R_3 = H$
3 $R_1 = R_2 = CH_3, R_3 = H$
4 $R_1 = OMe, R_2 = H, R_3 = t\text{-}Bu$

5 $R_1 = CH_3, R_2 = R_3 = H, R_4 = H$
6 $R_1 = R_2 = CH_3, R_3 = H, R_4 = CH_2CH_2OH$
7 $R_1 = OMe, R_2 = H, R_3 = t\text{-}Bu, R_4 = H$

2. Results

The relative disposition of the carbonyl group of the phenyl-amide moiety (PhNHCO) regarding the 2-substituent in the phenyl ring, as a plane of reference, gives rise to several conformers: antiperiplanar (*ap*), anticlinal (*ac*), synclinal (*sc*) and synperiplanar (*sp*), in agreement with the torsion angle C2–C1–N7–C8 values of ±180–150°, ±150–90°, ±90–30° and ±30–0°, respectively. In Fig. 1 are shown the Newman projections along the C1–N7 bond.[11]

In both *syn*-conformers, the PhNHCO carbonyl is pointing towards the 2-substituent, thus *endo* positioned with regard to

Exo *Endo*

Antiperiplanar (*ap*) Anticlinal (*ac*) Synclinal (*sc*) Synperiplanar (*sp*)

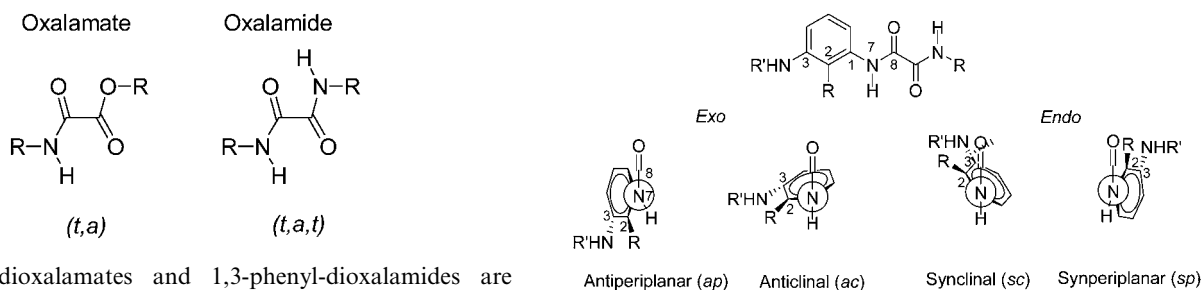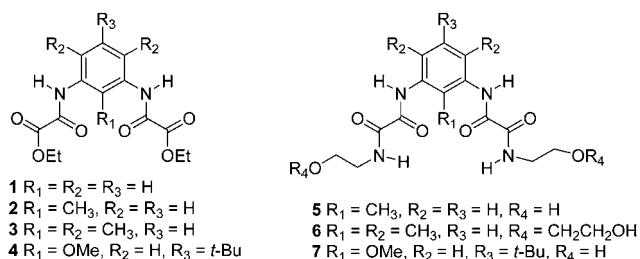**Fig. 1** Newman projections of conformers derived from the C2–C1–N7–C8 torsion angle, viewed along the C1–N7 bond.

the cavity, whereas the *anti*-conformers are *exo* positioned. Taking into account the two arms, ten combinations are possible: three *exo–exo* (*ap–ap*, *ac–ac*, *ap–ac*), four *exo–endo* (*ap–sc*, *ap–sp*, *ac–sc*, *ac–sp*) and three *endo–endo* (*sc–sc*, *sc–sp*, *sp–sp*).

There are two reported polymorphs of diethyl 1,3-phenyl-dioxalamate **1**[10b] and **1**'.[10c] In the conformation exhibited by polymorph **1**, both amide carbonyls are located pointing *endo* to the cavity and *syn* (*sc–sp*) positioned regarding to the phenyl ring with C2–C1–N7–C8 and C1–N7–C8–O8 torsion angles of 37.0(3)° and −4.1(3)°, respectively. This conformation allows a full intramolecular hydrogen bonding scheme combining one O⋯H2⋯O three centred and two NH⋯O hydrogen bonding interactions, respectively. Thus a set of four adjacent intramolecular rings are formed, which are described by the graph set notation[12] as [$S(5)S(6)S(5)S(6)$] motif. Meanwhile in **1**', the torsion angles C6–C1–N7–C8 and C1–N7–C8–O8 take values of 32.6(5)° and 179.3(3)°, respectively, in agreement with an *exo* (*ac*)–*exo*(*ac*) conformation of both oxalamate arms. This conformation favors the formation of two sets of intramolecular six and five membered hydrogen bond motifs [$S(6)S(5)$]. A common feature of conformers **1** and **1**' is the twist of both oxalamate side arms, one of them tilted up and the other tilted down with regard to the mean plane of the phenyl ring. The out-of-plane conformation is characteristic of disubstituted ethyl *o*- and *p*-phenyl-bis-oxalamates,[13] in contrast with the reported planar conformation of monosubstituted ethyl *N*-phenyl oxalamate.[14]

1 **1'**
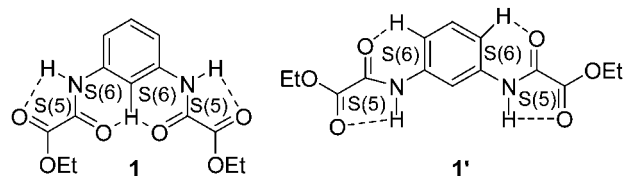
2.1 Intramolecular hydrogen bonding and molecular structure

Oxalamates 2–4 in the solid state. The molecular structures and intramolecular hydrogen bonding schemes of compounds **2–4** are shown in Fig. 2 and a summary of bond lengths and angles is listed in Table 1. The OC–CO distances are similar to the reported structure of diethyl 1,3-phenyl-dioxalamate **1** in agreement with OC–CO single bond and *anti* disposition between amide and ester carbonyls in both oxalamate arms. In compounds **2–4**, the amide proton is located *trans* to the amide

Table 1 Selected bond lengths (Å) and angles (deg) of compounds **2–7**[a]

Compounds	2	3	4	5	6	7
Atoms				Bond lengths/Å		
C1–N7	1.431(3)	1.417(5)	1.402(4)	1.440(6)	1.441(3)	1.409(3)
C3–N17	1.433(3)	1.429(5)	1.413(4)	1.415(6)		1.397(3)
N7–C8	1.335(3)	1.344(5)	1.345(4)	1.324(6)	1.317(4)	1.344(3)
N10–C9				1.317(6)	1.313(5)	1.319(3)
N17–C18	1.335(3)	1.331(5)	1.342(4)	1.338(6)		1.353(3)
N20–C19				1.337(6)		1.330(4)
C8–C9	1.535(3)	1.532(6)	1.529(4)	1.505(7)	1.525(5)	1.538(4)
C18–C19	1.543(3)	1.524(6)	1.543(5)	1.517(6)		1.527(4)
Atoms				Torsion angles/°		
C2–C1–N7–C8	64.4(3)	−60.4(5)	179.5(3)	−126.5(5)	−72.4(4)	−176.1(3)
C2–C3–N17–C18	67.4(3)	−103.5(4)	−178.4(3)	−144.5(4)		−177.6(3)
C6–C1–N7–C8	−117.0(2)	123.4(4)	0.3(5)	55.4(7)	108.0(3)	−4.9(5)
C1–N7–C8–O8	−0.2(4)	−9.5(6)	−3.6(5)	−1.2(9)	10.3(6)	−2.3(5)
C4–C3–N17–C18	−113.7(2)	76.5(4)	0.8(5)	38.5(7)		−1.6(5)
C3–N17–C18–O18	−0.8(3)	−2.1(6)	−4.5(5)	1.8(8)		2.5(5)
O8–C8–C9–O9	−167.9(2)	165.0(4)	−176.1(3)	−169.1(5)	179.1(3)	179.7(3)
O18–C18–C19–O19	−177.3(2)	168.6(4)	−177.4(4)	−179.6(4)		178.0(3)
N7–C8–C9–X10	−169.14(18)	170.0(3)	−178.6(3)	−165.1(5)	176.3(3)	−179.7(2)
N17–C18–C19–X20	179.97(18)	169.9(3)	−178.1(3)	−177.2(4)		177.7(2)
N10–C11–C12–O13					−177.3(3)	−59.5(3)
N20–C21–C22–O23						66.2(3)
O13–C14–C15–O16					69.1(4)	

[a] X = O in **2–4** and X = N in **5–7**.

carbonyl as in most secondary amides. The amide and ester carbonyls are *anti* to each other with similar O8=C8–C9=O9 and O18=C18–C19=O19 torsion angle values between ±165 and ±178°. The N7–C8–C9–O10 and N17–C18–C19–O20 torsion angle values are near to 180°, in close agreement with those values reported for diethyl phenyl-dioxalamates.[10]

The introduction of a CH₃ group in the C-2 position, compound **2**, increases the twisting out of the ethyl oxalamate arms from 37.0(3)° in polymorph **1** to 64.4(3) and 67.4(3)° (C2–C1–N7–C8 and C2–C3–N17–C18 torsion angles, respectively), as reported for diamides derived from 2-methyl-benzene-1,3-diamine.[15] Thus both oxalamate arms are toward one another, one above the plane of the phenyl ring and the other below this plane with both amide carbonyls in synclinal (*sc*) disposition in relation to the phenyl ring, but even *endo* to the cavity. This conformation allows the formation of a set of four adjacent intramolecular rings [S(5)S(7)S(7)S(5)] with the participation of NH and C2–CH₃ hydrogen atoms as donors and both carbonyls as acceptors: N7–H7···O9, N17–H17···O19, C23–H23A···O18 and C23–H23B···O18, Fig. 2(a). It is worthy to note that, in this compound and in related diamides, the methyl group is pointing towards the amide carbonyl thus favoring the S(7) ring, whereas in monoamides derived from *o*-tolylamine[16] it is always in the opposite direction. In spite of the steric requirements of the C2–CH₃ group, this conformer strongly resembles that of polymorph **1**, where the central S(6) intramolecular hydrogen bonded rings are substituted by larger S(7) ring motifs. In Table 2 the geometric parameters associated with intramolecular hydrogen bonding of compounds **2–4** are summarized. The interaction lengths are shorter than the sum of the van der Waals radii of the atoms involved (H = 1.20, C = 1.70, N = 1.55, O = 1.50 Å).[17]

Further increasing the steric restraints with CH₃ substituent groups in C2, C4 and C6, compound **3**, the oxalamate arms

become twisted by −60.4(5)° and −103.5(4)° for C2–C1–N7–C8 and C2–C3–N17–C18 torsion angles, respectively. This result is in agreement with the mean value of *ca.* 70° reported for 2,4,6-trimethyl-benzene-1,3-diamine.[18] The oxalamate arms are also up and down, adopting a synclinal (*sc*) and anticlinal (*ac*)
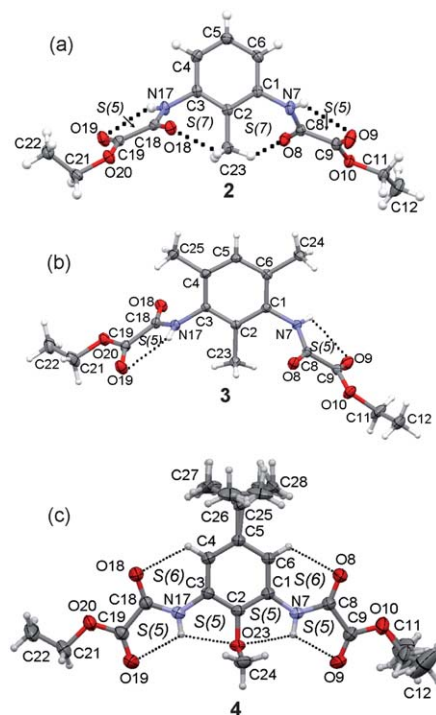

Fig. 2 Molecular structure at 30% probability level and intramolecular interactions of dioxalamates **2–4**.

Table 2 Geometric parameters of intramolecular interactions in compounds **2–7**[a]

Comp.	D–H···A	D–H/Å	H···A/Å	D···A/Å	D–H···A/°	HB motif
2	N7–H7···O9	0.86	2.31	2.696(3)	107	S(5)
	N17–H17···O19	0.86	2.31	2.693(2)	107	S(5)
	C23–H23A···O18	0.96	2.44	3.156(3)	131	S(7)
	C23–H23B···O8	0.96	2.58	3.115(3)	115	S(7)
3	N7–H7···O9	0.86	2.39	2.727(4)	104	S(5)
	N17–H17···O19	0.86	2.37	2.728(4)	105	S(5)
4	N7–H7[a]···O9	0.86	2.20	2.640(4)	111	S(5)
	N7–H7[a]···O23	0.86	2.27	2.694(3)	110	S(5)
	N17–H17[b]···O19	0.86	2.25	2.678(4)	111	S(5)
	N17–H17[b]···O23	0.86	2.25	2.703(4)	110	S(5)
	C4–H4···O18	0.93	2.34	2.940(4)	122	S(6)
	C6–H6···O8	0.93	2.37	2.967(4)	121	S(6)
5	N7–H7···O9	0.86	2.26	2.659(5)	109	S(5)
	N10–H10···O8	0.86	2.39	2.749(5)	106	S(5)
	N17–H17···O19	0.86	2.25	2.670(5)	110	S(5)
	N20–H20···O18	0.86	2.36	2.727(5)	106	S(5)
	C4–H4···O18	0.93	2.51	2.977(6)	111	S(6)
6	N7–H7···O9	0.86	2.29	2.675(3)	107	S(5)
	N10–H10···O8	0.86	2.32	2.701(4)	107	S(5)
7	N7–H7···O9[c]	0.86	2.20	2.647(3)	112	S(5)
	N7–H7···O24[c]	0.86	2.27	2.692(3)	110	S(5)
	N10–H10···O8	0.86	2.33	2.714(3)	107	S(5)
	N17–H17···O19[d]	0.86	2.24	2.665(3)	110	S(5)
	N17–H17···O24[d]	0.86	2.30	2.704(3)	109	S(5)
	N20–H20···O18	0.86	2.32	2.693(3)	106	S(5)
	C4–H4···O18	0.93	2.30	2.912(3)	123	S(6)
	C6–H6···O8	0.93	2.38	2.974(3)	121	S(6)

[a] $\Sigma \angle$ N7H7/° = 359 (a), 360 (c); $\Sigma \angle$ N17H17/° = 360 (b), 359 (d).

disposition, in relation to the mean plane of the phenyl ring, and *endo–exo* positioned to the cavity. Intramolecular hydrogen bonding is reduced to only two S(5) ring motifs, formed by N7–H7···O9 and N17–H17···O19 interactions, Fig. 2(b).

In compound **4**, the bulkiest OCH$_3$ substituent in C2 leads to the full rotation of both oxalamate side arms to locate them almost in the same plane of the phenyl ring, C2–C1–N7–C8 and C2–C3–N17–C18 torsion angles of 179.5(3)° and −178.4(3)°, as found in diamides derived from 2-methoxy-5-methyl-benzene-1,3-diamine,[19] both adopting an antiperiplanar (*ap*) disposition, in relation to the mean plane of the phenyl ring and *exo–exo* positioned to the cavity. In this molecule the *t*-Bu substituent is far away from the cavity, thus the steric effect is mainly exerted by the methoxy group. The OMe group is almost perpendicular to the phenyl ring (C1–C2–O23–C24 = 91.3(3)°) leading the oxygen atom in the same plane. This conformation is probably assisted by cooperative intramolecular hydrogen bonding.[20] The amide hydrogen atoms are involved in a three-centred hydrogen bonding with both O-atoms from the ester carbonyl and methoxy groups (O9···H7···O23 and O19···H17···O23), an important feature of this interaction is that the sum of angles around the amide H-atom ($\Sigma \angle$NH) is close to 360°.[21] In the opposite side, the amide carbonyls are also interacting with the aromatic hydrogen atoms H4 and H6 (C4–H4···O18 and C6–H6···O8). The full system is composed of six adjacent rings described by the graph set notation as an [S(5)S(6)S(5)S(5)S(6)S(5)] ring system, Fig. 2(c).

Oxalamides 5–7 in the solid state. Dioxalamides **5–7** are symmetrical but each arm is composed of two different amide groups, one of them directly linked to the phenyl ring (PhNHCO)

and the other to an ethylamine residue (RNHCO). The molecular structures and intramolecular hydrogen bonding schemes of compounds **5–7** are shown in Fig. 3 and a summary of bond
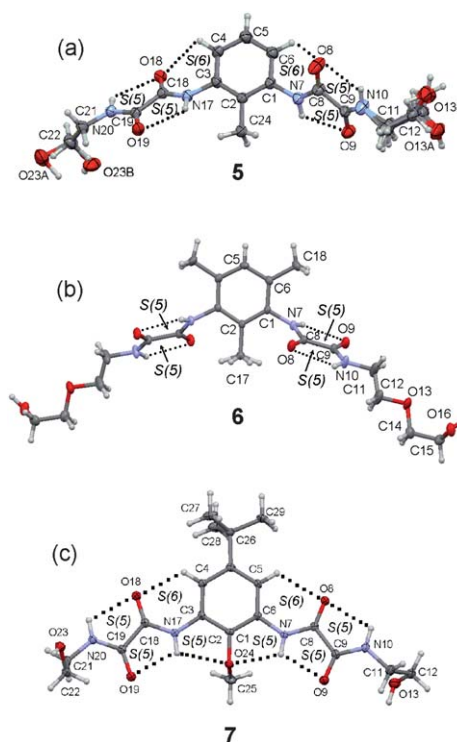

Fig. 3 Molecular structure at 30% probability level and intramolecular interactions of dioxalamides **5–7**.

lengths and angles is listed in Table 1. The OC–CO distances are similar to the reported structures of phenyl oxalamides[22] in agreement with OC–CO single bond. As in most of secondary oxalamides, both amide groups are *anti* to each other with N7–C8–C9–N10 and N17–C18–C19–N20 torsion angles between ±165 and ±180°.

In compound **5**, both oxalamide side arms are almost planar with C1–N7–C8–O8 and C3–N17–C18–O18 torsion angles close to 0°. Phenylamide carbonyls (C8=O8 and C18=O18) are both *exo* positioned to the cavity and anticlinal (*ac*) to the mean plane of the phenyl ring, one of them above and the other below the phenyl ring plane with C2–C1–N7–C8 and C2–C3–N17–C18 torsion angles of −126.5(5)° and −144.5(4)°, respectively. This last conformation brings about the formation of intramolecular C4–H4···O18 HB, S(6) ring, at the expense of two S(7) rings in the parent oxalamate **2**. In addition N7–H7···O9, N10–H10···O8, N17–H17···O19 and N20–H20···O18 hydrogen bonding, typical of oxalamides, are observed. Therefore, the intramolecular hydrogen bonding pattern is depicted by two sets of adjacent HB ring systems [S(5)S(5)S(6)] and [S(5)S(5)], Fig. 3(a).

Compound **6** has a crystallographic plane of symmetry and thus only one half of the molecule is observed. The fragment N–CO–CO–N of the oxalamide arms is almost planar with C1–N7–C8–O8 and N10–C11–C12–O13 torsion angles of 10.3(6)° and −177.3(3)°, respectively. The OH group at the end of the arm is in a *gauche* conformation with O13–C14–C15–O16 torsion angle of 69.1(4)°. Both arms are synclinarly (*sc*) positioned with respect to the mean plane of the phenyl ring, with C2–C1–N7–C8 torsion angle of −72.4(4)° and the phenylamide carbonyl pointing towards the cavity. The intramolecular HB scheme is described as two sets of [S(5)S(5)] ring systems, Fig. 3(b).

The conformation of oxalamide **7** strongly resembles the conformation observed for the parent oxalamate **4**: the oxalamide arms are *ap* to the phenyl ring (C2–C1–N7–C8 = −176.1(3)° and C2–C3–N17–C18 = −177.6(3)°), both are *exo* disposed to the cavity and the OMe group is almost perpendicular to the phenyl ring (C1–C2–O24–C25 = 88.6(3)°). The OH group at the end of the arm is in a *gauche* conformation with N10–C11–C12–O13 and N20–C21–C22–O23 torsion angles of −59.5(3)° and 66.2(3)°, respectively, Fig. 3(c).

The substitution of EtO in oxalamates **2–4** for RNH in oxalamides **5–7** increases the intramolecular HB, allowing the formation of an additional S(5) ring in each arm due to the (*t,a,t*) conformation of the dioxalamide RHN–CO–CO–NHPh fragment. Therefore, the following patterns are observed: [S(5)S(5)S(6)] and [S(5)S(5)] for **5**, two sets of [S(5)S(5)] rings for **6** and eight adjacent rings [S(5)S(5)S(6)S(5)S(5)S(6)S(5)S(5)] for **7**. At this point it is worthy to note that the C1–N7/C3–N17 distances enlarge when the oxalyl arm is out of the mean plane of the phenyl ring. This result is consistent with the C1–N7 distance value of 1.414 Å measured in planar *N,N'*-bis(3,5-dimethyl-phenyl)oxalamide,[13] similar to the C1–N7/C3–N17 distance values observed in the corresponding in plane arm of compounds **3–5** and **7**. In contrast, a C1–N7 distance value of 1.435 Å has been measured in the almost perpendicular *N,N'*-bis-(2,4,6-tri-methyl-phenyl)oxalamide,[13] in agreement with C1–N7/C3–N17 distance values observed in the corresponding out of plane arm of compounds **2**, **3**, **5** and **6**.

Gas phase structure of 2–7. *Ab initio* theoretical calculations performed in diethyl *N,N'*-[1,3-phenyl]dioxalamate have pointed out that the conformer *exo*(*ap*)–*exo*(*ap*), polymorph **1'**, is more stable than the *endo*(*sp*)–*endo*(*sp*) conformer, polymorph **1**, just by 1.0–2.0 kcal mol⁻¹, this energy becomes smaller when acetone is included as a solvent.[10a,23] This small difference in energy has been used to explain the occurrence of both polymorphs. In order to gain more information about the preferred conformation and the intramolecular hydrogen bonding interactions, density functional theoretical (DFT) calculations were performed in compounds **2–7**. The *exo*(*ap*)–*exo*(*ap*) conformer is predicted as the most stable for compounds **2**, **4**, **5**, and **7**. In the case of compound **2** and its derived oxalamide **5**, DFT calculations do not agree with XRD. Compound **2** showed two energy minima, one of which correspond to the conformer *exo*(*ap*)–*exo*(*ap*) with C2–C1–N7–C8 and C2–C3–N17–C18 torsion angles very close to 180° and the other corresponding to the conformer *endo*(*sc*)–*endo*(*sc*) with C2–C1–N7–C8 and C2–C3–N17–C18 torsion angles of 59.9° and 66.7°, respectively. The energy difference between both conformers is 5.7 kcal mol⁻¹ in favor of the *exo*(*ap*)–*exo*(*ap*) conformer, larger than the conformational barrier of 4.4 kcal mol⁻¹ reported for compound **1**.[10a] This gap in energy is expected because of the steric restraints to rotation imposed by C2-Me group. It is worthy to mention that this last conformer has the largest dipole moment of 4.07 Debyes, against 0.29 Debyes shown by the conformer *endo*(*sc*)–*endo*(*sc*). The amide N atom bears a positive formal charge (0.201) in the *exo*(*ap*)–*exo*(*ap*) conformer and a negative formal charge (−0.152 and −0.149) in the *endo*(*sc*)–*endo*(*sc*) conformer, in agreement with the absence of the N lone pair conjugation into the phenyl ring in the last conformer.

When the steric effect is increased by substitution in C4 and C6 positions, compounds **3** and **6**, both oxalamate groups are tilted out of the phenyl mean plane to give conformers very similar to those found by X-ray. In compound **3**, the conformers *endo*(*sc*)–*endo*(*sc*), *exo*(*ac*)–*exo*(*ac*) and *exo*(*ac*)–*endo*(*sc*) (from XRD) were tested, this last one is more stable than the other two by 1.8 and 1.1 kcal mol⁻¹, respectively. In the case of oxalamide **6**, the *endo*(*sc*)–*endo*(*sc*) conformer was the predicted one, in close agreement with the XRD structure. The calculated planar *exo*(*ap*)–*exo*(*ap*) conformers of **4** and **7** are in close agreement with XRD structures. In both cases, the N atoms bear a positive formal charge as a consequence of the conjugation of the lone pair of electrons into the phenyl ring. The optimized structures and formal charges are shown in Fig. 4. The *exo*(*ap*)–*exo*(*ap*) conformation is more stable than the other conformations due to the conjugation that stabilizes the molecule and minimizes the conformational energy.

Hydrogen bonding in solution by ¹H NMR. At this point the question remains whether, in the case of compounds **4** and **7**, the observed conformers are the result of the minimization of electronic repulsive interactions between amide and OMe oxygen atoms or hydrogen bonding interactions. To address this issue, the dependences of the chemical shift with temperature ($\Delta\delta/\Delta T$) of the amide protons were measured in DMSO-d_6 solutions. This coefficient has been routinely used to estimate the proton mobility and the thermodynamic parameters associated with intra or intermolecular hydrogen bonding formation.[22–24] In
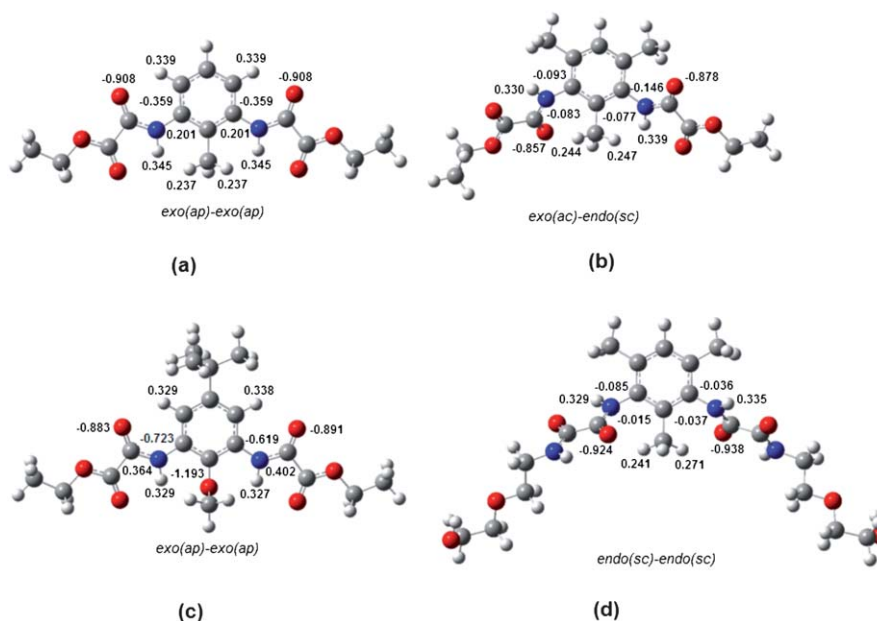
Fig. 4 Molecular structures and charges of the most stable optimized conformers of compounds **2** (a), **3** (b), **4** (c) and **6** (d) at DFT/PBEPBE 6-31+G (3df, 3pd) level of theory.

amides, $\Delta\delta NH/\Delta T$ values smaller than 3.0 ppb K^{-1}, in DMSO, are associated with low mobility protons and thus indicate a strong intramolecular hydrogen bond. Another indicator of low mobility is a small difference between chemical shifts measured in DMSO-d_6 and CDCl$_3$ solutions ($\Delta\delta NH$). In Table 3 are summarized the relevant ^1H NMR data of compounds **1–7**. The chemical shifts of the N*H*Ph signals of compounds **1–7** in DMSO-d_6 appear in the range of 10.8 to 9.9 ppm, in agreement with their more acidic character than the N*H*R signals, in compounds **5–7**, which are at lower frequencies, 9.0–8.8 ppm. Nevertheless $\Delta\delta NH/\Delta T$ values of both amide protons indicate moderate intramolecular hydrogen bonding in compounds **1–4** and **6**. It is worthy to note that the mobility of the N*H*Ph proton is increased in oxalamide **5** ($\Delta\delta NHPh = -9.3$ ppb K^{-1}) in comparison with its parent oxalamate **2** ($\Delta\delta NHPh = -4.7$ ppb K^{-1}), in agreement with more intermolecular hydrogen bonding character in **5**. In contrast, intramolecular hydrogen bonding is strengthened in oxalamide **7** if compared to its parent oxalamate **4**. Actually, the $\Delta\delta NHPh/\Delta T$ value of -2.0 ppm K^{-1}, in the former, is in agreement with strong intramolecular three-centred

hydrogen bonds O9···H7···O23···H17···O19. The corresponding value in compound **4** is in accordance with moderate intramolecular hydrogen bonding but the smallest $\Delta\delta NHPh$ value indicates the lowest mobility among the oxalamates **1–4**. Besides, the IR vibrational frequency of N*H*Ph is shifted from 3378 cm^{-1} in **4** to 3357 cm^{-1} in **7** as reported for three-centred hydrogen bonded oxalamates[25] and bisoxalamides.[22] These results confirm that the same scheme of intramolecular hydrogen bonding found by XRD in compounds **4** and **7** is persistent in solution and thus the hydrogen bonding nature of the observed conformation.

2.3 Crystal packing and supramolecular arrangement

Compounds **2** and **3** crystallize as monoclinic systems, space group $P2_1/c$ with four molecules in the unit cell, compounds **4** and **5** as triclinic, space group $P\bar{1}$ with two molecules in the unit cell, whereas compounds **6** and **7** crystallize as monoclinic, space group $C2/c$ with four molecules in the unit cell. Compound **7** is a special case in which the monoclinic structure has a β angle indistinguishable from 90.0°. The geometric parameters associated with intermolecular non-covalent interactions D–H···A are summarized in Table 4. In order to avoid data duplication, the reader is referred to the corresponding entry. Classic hydrogen bonding[26] and C–H···O[27] or C–H···π[28] interactions are in agreement with accepted criteria. Classification and geometry of CO···CO interactions[29] and π-stacking[30] are in accordance with accepted values.

Oxalamates 2–4. The zero dimensional array (0-D) of compound **2** is given by pairing of two centrosymmetric molecules through self-complementary strong N17–H17···O8^{ii} hydrogen bonding, with the participation of the amide group as both hydrogen donor and acceptor. Intercentroid and interplanar distances of 4.5642(14) and 3.6254(9) Å, respectively,

Table 3 δX^1H and $\Delta\delta X^1H/\Delta T$ NMR data (X = N, O) of compounds **1–7** in DMSO-d_6^{a}

	Compound						
Parameter	**1**	**2**	**3**	**4**	**5**	**6**	**7**
$\delta NHPh$	10.82	10.48	10.37	10.04	10.29	10.25	9.90
$\Delta\delta NHPh^a$	1.89	1.62	1.90	0.79			
$\Delta\delta NHPh/\Delta T$	−5.50	−4.70	−5.21	−4.20	−9.30	−5.39	−2.00
δNHR					8.81	8.80	8.97
$\Delta\delta NHR/\Delta T$					−4.96	−5.50	−4.9
δOH					n.o.	4.65	n.o.
$\Delta\delta OH/\Delta T$						−5.43	

^{a} $\delta^1H_{DMSO-d_6} - \delta^1H_{CDCl_3}$ available only for **1–4** for solubility restrictions.

suggest a parallel displaced $pd–\pi\cdots\pi^{ii}$ stacking interaction between phenyl rings (symmetry code ii: $1 - x$, $-y$, $1 - z$). The resulting ring motif $R_2^2(16)$ is developed into 1-D columns by self-complementary amide N7–H7$\cdots$O18^i hydrogen bonding interactions, which describe a second $R_2^2(16)$ ring motif. In addition, two π-interactions strengthen the column assembly: N7–H7$\cdots\pi^i$ and $pd–\pi$-stacking^i, this last with 4.5383(14) and 3.5815(9) Å of intercentroid and interplanar distances (i: $2 - x$, $-y$, $1 - z$). The whole 1-D array is depicted as a column developed by antiparallel $C_2^2(8)[R_2^2(16)\ R_2^2(16)]$ chains (second level graph set descriptor) developing along the direction of the a axis, Fig. 5. The second dimension (2-D) is arranged by C11–H11A$\cdots$O18^{iii} soft interactions that link the columns forming $R_2^2(24)$ ring motifs along the direction of the c axis (iii: $2 - x$, $-y$, $2 - z$).

Compound **3** also forms amide-linked centrosymmetric dimers, as in **2**, through the ac-oxalamate side arm N17–H17$\cdots$O8^v (v: $1 - x$, $-y$, $-z$) to define a $R_2^2(16)$ ring motif. In this case each dimer is connected with four other dimers through N7–H7$\cdots$O18^{iv} hydrogen bonding and C24–H24C$\cdots$O18^{iv} interaction, to form $R_2^1(7)[C(8)C(9)]$ second level ring motif (iv: x, $\frac{1}{2} - y$, $-\frac{1}{2} + z$). This arrangement, viewed in the bc plane, looks like a brick wall-sheet of alternating squared $R_2^2(16)$ and hexagon $R_6^6(32)$ ring motifs, Fig. 6. The $R_2^2(16)$ dimers are $pd–\pi$-stacked^{vi} as the intercentroid and interplanar distances of 4.540(2) and 3.6204(13) Å (vi: $2 - x$, $-y$, $-z$), respectively, indicate.

The extended embrace disposition of **4** and the steric hindrance of the C2-OMe group do not allow intermolecular hydrogen bonding. However, dipolar carbonyl–carbonyl and π-stacking interactions direct the formation of centrosymmetric pairs. Two self-complementary sheared parallel carbonyl–carbonyl interactions are formed: C8=O8$\cdots$C19^{viii} [O8$\cdots$C19 = 3.270(4) Å, C8=O8$\cdots$C19 = 104.7(3)°] and C18=O18$\cdots$C9^{viii}
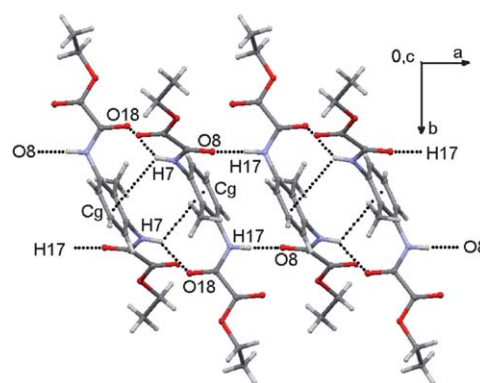

Fig. 5 1-D columns along the a axis formed by N–H$\cdots$O, N–H$\cdots\pi$ and pd–π-stacking interactions in compound **2**.

[O18$\cdots$C9 = 3.144(4) Å, C18=O18$\cdots$C9 = 101.9(3)°]. Intercentroid and interplanar distances of 3.7950(18) Å and 3.4580(13) Å, respectively, are in agreement with face to face π-stacking^{viii} ($viii$: $-x$, $-y$, $1 - z$), Fig. 7(a). These pairs are linked through weak C24–H24C$\cdots$O9^{vii} interactions with the participation of the methyl group from OMe as the donor and ester carbonyl as the acceptor (vii: $-x$, $1-y$, $1 - z$). Thus $R_2^2(18)$ ring motifs are outlined developing 1-D zig-zagging tapes along the direction of the a axis. If intramolecular HB is included, $[S(5)S(5)]$ motifs, chair like H$_4$O$_4$, octagons are also observed, Fig. 7(b). T-Shaped C21–H21B$\cdots\pi^{ii}$ interactions, $R_2^2(14)$ motif, are responsible to generate 2-D walls in the direction of the c axis.

Oxalamides 5–7. The typical $R_2^2(10)[R_2^2(16)\ R_2^2(24)]$ ring motif, in which the *anti* network is used, gives rise to hydrogen

Table 4 Geometric parameters of intermolecular interactions in compounds **2–7**^{a}

Comp.	D–H$\cdots$A	D–H/Å	H$\cdots$A/Å	D$\cdots$A/Å	D–H$\cdots$A/°	HB motif
2	N7–H7$^a\cdots$O18^i	0.86	2.39	3.074(2)	137	$R_2^2(16)$
	N7–H7$\cdots\pi^i$	0.86	3.18	3.710(2)	123	$R_2^2(6)$
	N17–H17$^b\cdots$O8^{ii}	0.86	2.32	2.995(2)	136	$R_2^2(16)$
	C11–H11A$\cdots$O18^{iii}	0.97	2.59	3.433(3)	145	$R_2^2(24)$
3	N7–H7$^c\cdots$O18^{iv}	0.86	2.24	3.060(4)	160	$C(8)$
	C24–H24C$\cdots$O18^{iv}	0.96	2.52	3.281(4)	136	$C(9)$
	N17–H17$^d\cdots$O8^v	0.86	2.15	2.903(4)	149	$R_2^2(16)$
4	C24–H24C$\cdots$O9^{vii}	0.96	2.41	3.348(5)	167	$R_2^2(18)$
	C21–H21B$\cdots\pi^{ii}$	0.96	2.85	3.668(4)	142	$R_2^2(14)$
5	N7–H7$^e\cdots$O18^{viii}	0.86	2.18	2.937(5)	146	$R_2^2(16)$
	N10–H10$^f\cdots$O8^{ix}	0.86	2.19	2.969(6)	151	$R_2^2(10)$
	N17–H17$^g\cdots$O19^x	0.86	2.20	2.932(5)	142	$R_2^2(10)$
	N20–H20$\cdots$O9^{viii}	0.86	2.49	3.306(4)	159	$R_2^2(24)$
6	N7–H7$^h\cdots$O16^{xi}	0.86	2.12	2.928(4)	157	$R_2^2(30)$
	N10–H10$^i\cdots$O8^{xii}	0.86	2.07	2.888(4)	158	$R_2^2(10)$
	O16–H16$\cdots$O9^{xiii}	0.84	1.97	2.798(3)	167	$R_2^2(34)$
7	N10–H10$^j\cdots$O13^{xiv}	0.86	2.40	3.139(3)	144	$R_2^2(10)$
	O13–H13$\cdots$O19^{xiii}	0.84	2.08	2.893(3)	164	$R_2^2(30)$
	C25–H25A$\cdots$O9^{xiii}	0.96	2.53	3.274(4)	134	$R_2^2(18)$
	C22–H22A$\cdots$O8^{xv}	0.97	2.46	3.279(3)	142	$C(13)$
	O23–H23$\cdots$O9^{xvi}	0.84	2.03	2.817(3)	156	$C(15)$
	N20–H20$^k\cdots$O23^{xvii}	0.86	2.14	2.922(3)	150	$R_2^2(10)$
	C27–H27B$\cdots$O24^{xvii}	0.96	2.55	3.377(4)	144	$R_2^2(16)$

^{a} $\Sigma\angle$N7H7/° = 332 (a), 351 (c), 355 (e), 349 (h); $\Sigma\angle$N17H17/° = 332 (b), 348 (d), 354 (g); $\Sigma\angle$N10H10/° = 356 (f), 360 (i), 342 (j); $\Sigma\angle$N20H20/° = 357 (k). Symmetry codes: (i) = $2 - x$, $-y$, $1 - z$; (ii) = $1 - x$, $-y$, $1 - z$; (iii) = $2 - x$, $-y$, $2 - z$; (iv) = x, $\frac{1}{2} - y$, $-\frac{1}{2} + z$; (v) = $1 - x$, $-y$, $-z$; (vi) = $2 - x$, $-y$, $-z$; (vii) = $-x$, $1 - y$, $1 - z$; ($viii$) = $-x$, $-y$, $1 - z$; (ix) = $-x$, $1 - y$, $-z$; (x) = $-1 - x$, $-y$, $1 - z$; (xi) = $\frac{1}{2} + x$, $\frac{1}{2} - y$, $\frac{1}{2} + z$; (xii) = $\frac{1}{2} - x$, $\frac{1}{2} - y$, $-z$; ($xiii$) = $-\frac{1}{2} - x$, $\frac{1}{2} - y$, $-z$; (xiv) = $-x$, $-y$, $-z$; (xv) = $-\frac{1}{2} + x$, $\frac{1}{2} + y$, z; (xvi) = $-\frac{1}{2} - x$, $\frac{1}{2} + y$, $\frac{1}{2} - z$; ($xvii$) = $-x$, y, $\frac{1}{2} - z$.
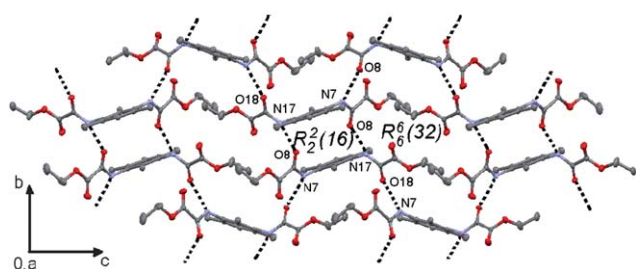
Fig. 6 View in the *bc* plane of a brick wall-sheet of alternating squared $R_2^2(16)$ and hexagon $R_6^6(32)$ like ring motifs, formed by N–H···O hydrogen bonding interactions in compound **3**.

bonded centrosymmetric dimers linked through two self complementary N–H···O interactions, N7–H7···O18^{viii} ($R_2^2(16)$) and N20–H20···O9^{viii} ($R_2^2(24)$), in compound **5**. In these motifs the hydrogen bonding donor NH and the acceptor CO belong to the same amide type, or amide-like interactions, that is phenyl-amide or hydroxyethylamide. The intercentroid distance of 4.986 (3) Å^{viii} between the phenyl spacers in the $R_2^2(16)$ motif is beyond the limit for a *pd*–π-stacking interaction. Each dimer is linked to other two also using the N–H···O *anti* network between the NH of phenylamide and the CO of hydroxyethylamide residue and conversely or amide-dislike interactions, forming two $R_2^2(10)$ ring motifs: N10–H10···O8^{ix} (*ix*: −*x*, 1 − *y*, −*z*) and N17–H17···O19^{x} (*x*: −1 − *z*, −*y*, 1 − *z*). The intermolecular spacing along these oxalamide motifs is 5.137(3) and 5.035(3) Å, respectively. The four N–H···O hydrogen bonds can be described, at the second level graph set descriptor, as two $C_4^4(16)[R_2^2(16)\ R_2^2(10)\ R_2^2(10)\ R_2^2(24)]$ chains running in the opposite direction, to
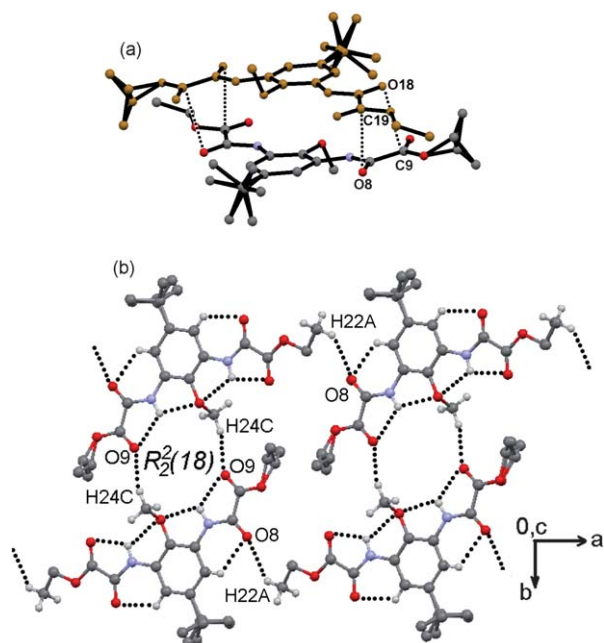
develop a rough sheet in the [2 8 11] mean plane. The whole crystal packing, Fig. 8(a), is strengthened by the cooperative participation of intramolecular hydrogen bonding *S*(5) motifs. Thus three centred hydrogen bonding O9···H7···O18 (Σ∠H7 = 355°) and O9···H20···O18 (Σ∠H20 = 354°) depict intra-dimers, and O8···H10···O8 (Σ∠H10 = 356°) and O19···H17···O19 (Σ∠H17 = 346°) inter-dimer H$_2$O$_2$ squares. The resulting $R_2^2(4)$ pattern is a common structural motif in oxalamide supramolecular architecture. In this molecule both ethanolamine residues are disordered. In one arm the residual ethanolamine fragment C11–C12–O13–H13 is moving in three positions with 24, 30 and 46 percent of occupancy and on the other arm, the residual hydroxyl group O23–H23 is moving in two positions with 51% (O23A) and 49% (O23B) percent of occupancy. For this last, the O23A···O23B distance of 2.810(3) Å was measured, in agreement with other similar structures^{9d} forming a $R_2^2(8)$ ring to reinforce 2-D, Fig. 8(b).

Molecule **6** is linked to other molecule, forming centrosymmetric pairs, by N10–H10···O8^{xii} (*xii*: ¹/₂ − *x*, ¹/₂ − *y*, −*z*), N7–H7···O16^{xi} (*xi*: ¹/₂ + *x*, ¹/₂ − *y*, ¹/₂ + *z*) and O16–H16···O9^{xiii} hydrogen bonding to form $R_2^2(16)[R_2^2(10)R_2^2(36)]$ ring motif. The intermolecular spacing along the oxalamide $R_2^2(10)$ motif is 5.060(3) Å. The propagation of these hydrogen bonding interactions along the (2 0 −2) direction gives rise to a *meso*-helix. The turn of the helix measures 18.0 Å between two phenyl rings, longer than 15.0 Å measured in the polymorph **1′**.^{10c} The *meso*-helix can be regarded as the alternate propagation of helical conformers of opposite chirality (M and P) around the inversion
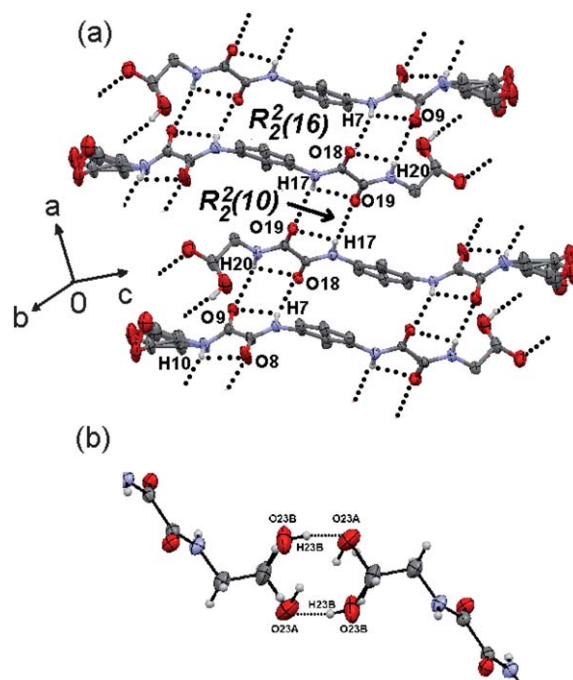

Fig. 7 Supramolecular structure of compound **4**. (a) Centrosymmetric pair linked by C=O···C=O dipolar and pd–π-stacking interactions (hydrogen atoms and *t*-Bu group are omitted for clarity). (b) 1-D zig-zagging tape linked through weak C24–H24C···O interactions along the *a* axis, chair like H$_4$O$_4$ octagons are also included.

Fig. 8 (a) Partial view of the rough complex sheet of compound **5**, developed by N–H···O and O–H···O hydrogen bonding interactions in the [2 8 11] mean plane (hydrogen atoms not involved in HB have been omitted for clarity). Oxalamide $R_2^2(10)$ and $R_2^2(16)$ ring motifs are clearly appreciated as well as disordered ethanolamine fragment C11–C12–O13–H13. (b) A detail of the disordered hydroxyl group O23–H23 showing the $R_2^2(8)$ ring motif through O–H···O interactions.

centre thus the twist sense changes every half-turn of the helix, Fig. 9(a). To the best of our knowledge compound **6** is the first example of helical 1,3-phenyl-dioxalamide. An infinite number of helixes are interlinked by O16–H16⋯O9^{xiii} (xiii: $-\frac{1}{2} - x$, $\frac{1}{2} - y$, $-z$) interactions through the ending ethanolamine OH and the ethanolamide CO, forming $R_2^2(34)$ ring motifs, which combined with the above mentioned N7–H7⋯O16 interactions depict a $R_2^2(7)[R_2^2(30)\ R_2^2(34)]$ second level ring motif. A view of the full set of hydrogen bonding motifs in the *ac* plane is shown in Fig. 9(b). H_2O_2 squares and H_4O_4 boat like octagons appear as intrahelix and interhelix motifs, when three-centred HB is considered: O8⋯H10⋯O8 ($\Sigma \angle H10 = 360°$) and O9⋯H7⋯O16 ($\Sigma \angle H7 = 349°$), respectively. Better appreciated is the 20-membered ring in the top view of the helix shown in Fig. 9(c). The whole 2-D architecture is composed of independent-weaving sheets propagating in the (2 0 −2) direction.

In molecule **7**, where the adopted conformation maximizes the intramolecular hydrogen bonding, also centrosymmetric dimers are formed by hydrogen bonding between one ending hydroxyl group and RNHCO amide carbonyl O13–H13⋯O19^{xiii}, and also by C25–H25A⋯O9^{xiii} soft interactions to form $R_2^2(16)[R_2^2(30)\ R_2^2(18)]$ second level ring motif. One dimension is generated by the propagation of this motif along the direction of the *b* axis through N10–H10⋯O13^{xiv} (xiv: $-x, -y, -z$) hydrogen bonding to form $R_2^2(10)$ ring motifs and C22–H22A⋯O8^{xv} (xv: $-\frac{1}{2} + x$, $\frac{1}{2} + y, z$) forming $C(13)$ chains, Fig. 10(a). The curvature of the assembly is inherently imprinted by the *exo–exo* symmetric disposition of the oxalamide arms. The remaining OH, NH and CO groups link the curved chains through O23–H23⋯O9^{xvi} (xvi: $-\frac{1}{2} - x$, $\frac{1}{2} + y$, $\frac{1}{2} - z$) and N20–H20⋯O23^{xvii} (xvii: $-x, y$, $\frac{1}{2} - z$) interactions, to form $C(15)$ and $R_2^2(10)$ ring motifs. The

second dimension is strengthened by the soft contact C27–H27B⋯O24^{xvii} between *t*-Bu and OMe groups, dipolar carbonyl–carbonyl and π-stacking interactions to form π-stacked pairs. Both π-stacked molecules are related by C_2 symmetry axis, in close similarity with the parent oxalamate **4**: two self-complementary sheared parallel carbonyl–carbonyl interactions C8=O8⋯C19^{xvii} [O8⋯C19 = 3.235(4) Å, C8=O8⋯C19 = 105.2(2)°], C18=O18⋯C9^{xvii} [O18⋯C9 = 3.284(4) Å, C18=O18⋯C9 = 100.4(2)°] and a face-to-face π-stacking^{xvii} with intercentroid and interplanar distances of 3.6756(17) and 3.3608(11) Å, respectively, Fig. 10(b). Thus the full architecture is seen, in the *bc* plane, as a wall formed by lines of molecules alternately linked only by HB and then by a combination of HB and π-stacking interactions, running along the (−1 0 14) direction, Fig. 10(c). Hydrophobic contacts among these blocks along the direction of the *a* axis are given between *tert*-butyl groups with C29⋯C29 distance of 4.184(4) Å.

3. Discussion

The lengthening of the C1–N7/C3–N17 bonds suggests that the twisted conformation breaks the conjugation between the phenyl ring and the amide bond and directs the two oxalyl arms one above and the other below the plane of the phenyl ring. The XRD conformations exhibited by compounds **2–7** are the result of maximization of intramolecular hydrogen bonding and C–H⋯OC interactions, both assisted by dipole–dipole interactions coming from favorable antiparallel arrangements of the local N–H⋯OC dipoles. The conformation of oxalamates **3** and **4** is reliable; it is almost the same in oxalamides **6** and **7**, whereas the conformation of oxalamate **2** does not remain in the
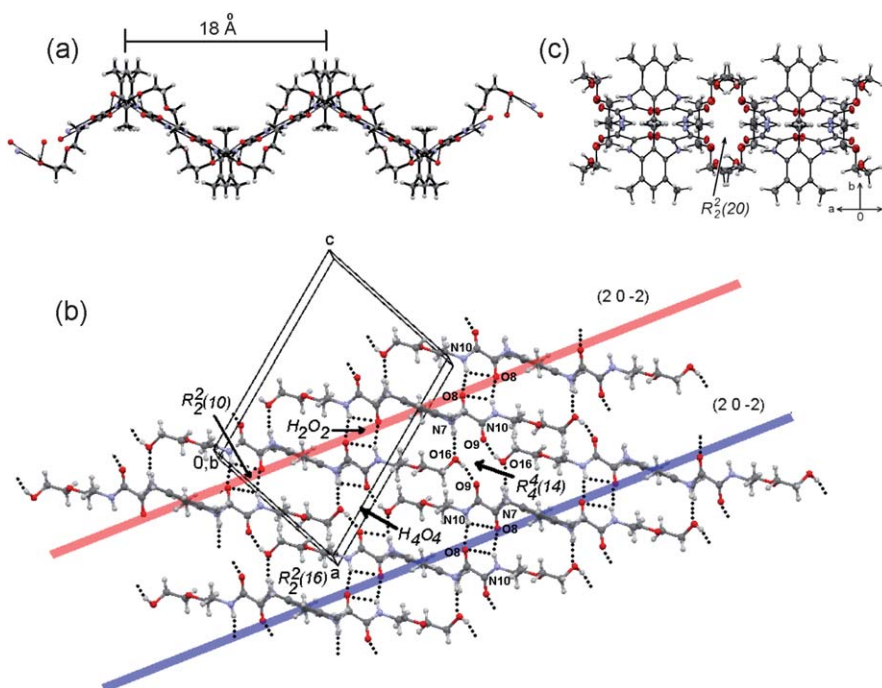

Fig. 9 (a) View of supramolecular *meso*-helix of compound **6**, hydrogen bonding interactions lie in the plane. (b) View of the full set of hydrogen bonding motifs in the *ac* plane: N10–H10⋯O8 ($R_2^2(10)$), N7–H7⋯O16 and O16–H16⋯O9, intrahelix H_2O_2 squares and interhelix H_4O_4 boat like octagons are highlighted. (c) Top view of $R_2^2(20)$ interhelical ring motif.
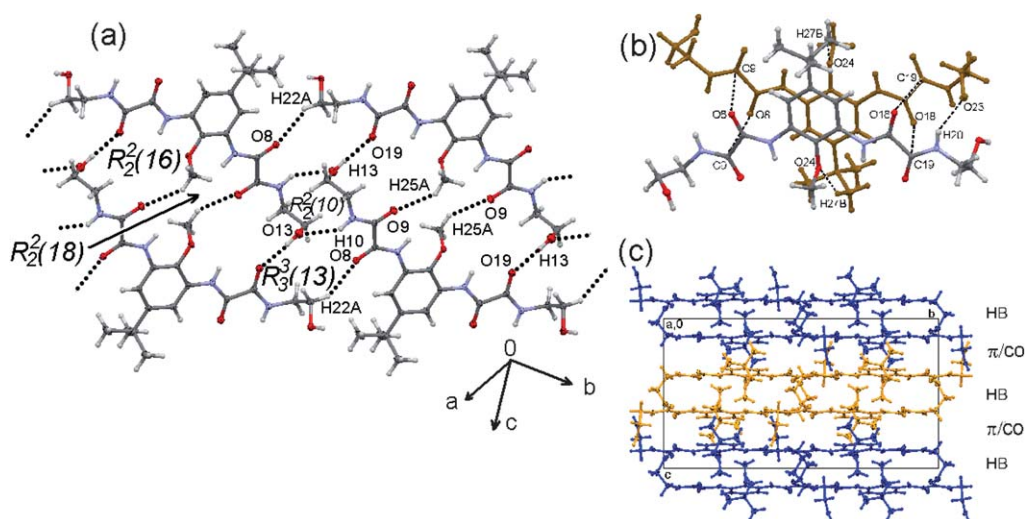
Fig. 10 (a) Supramolecular 1-D chains formed by O–H···O, N–H···O and C–H···O interactions along the *b* axis in compound **7**. (b) Molecular pair formed by C=O···C=O dipolar and face-to-face π-stacking interactions. (c) Full supramolecular architecture shown as a wall formed by lines of molecules alternately linked only by HB and then by a combination of HB and π-stacking interactions, running along the (−1 0 14) direction.

corresponding oxalamide **5**. The transformation of oxalamate into the corresponding oxalamide is accompanied with an increase in the hydrogen bonding capabilities. Intramolecular hydrogen bonding is increased by one S(5) ring motif per arm. The hydrogen bonding nature of the intramolecular O9···H7···O23···H17···O19 interactions in compound **7** was confirmed by $\Delta\delta\text{NHPh}/\Delta T$ measurements, with a value of −2.0 ppm K^{-1}.

Theoretical calculations predict the *exo*(*ap*)–*exo*(*ap*) conformer as the most stable in compounds **2**, **4**, **5** and **7** and conformer *endo*(*sc*)–*endo*(*sc*) in compounds **3** and **6** in agreement with the steric effects exerted by the substituents in the phenyl ring. Differences between theoretical predictions and XRD structures in compounds **2** and **5** can be attributed to intramolecular C–H···OC interactions which are strong enough to overcome the small energy difference between both conformers.

There is a clear trend, in the solid state, to adopt an *exo*(*ap*)–*exo*(*ap*) conformation by increasing the steric requirements of the C2-substituent. Further substitution in C4 and C6 leads to both oxalyl arms almost perpendicularly positioned to the phenyl ring resulting in a very reliable conformation also observed in diamides derived from 2,4,6-trimethyl-benzene-1,3-diamine.[18]

Intermolecular NH···O=C(amide) hydrogen bonds are preferred over NH···O=C(ester) as supramolecular synthons in the formation of crystal networks by dioxalamates **2** and **3**. This last interaction is exclusively used for intramolecular hydrogen bonding. Carbonyl amide groups are also differentially used for hydrogen bonding in oxalamides, NH···O=C amide dislike interactions are mainly used for intramolecular HB in oxalamides **5–7** and for supramolecular synthons only when also involved in intramolecular three-centred hydrogen bonding. NH···O=C amide-like interactions are exclusively used for intermolecular hydrogen bonding in compound **5**.

This set of compounds appears as centrosymmetric pairs in the 0-D which further develop 1-D as π-stacked columns, tapes, helix or chains. Walls or zig-zagging, rough or weaving sheets give shape to the 2-D. It is worthy to note that 0-D and 1-D arrays are directed by strong amide N–H···O self-complementary hydrogen

bonding in dioxalamates **2** and **3** whereas the 2-D is structured through weak C–H···O interactions. Hydroxyl combined with amide moieties are not enough to develop a strong 3-D in oxalamides **5** and **6**, although they show more complex networks in comparison with their parent oxalamates.

Instead of the characteristic $R_2^2(10)$ ring motif frequently observed in oxalamide and oxalamate supramolecular architectures, the $R_2^2(16)$ ring motif is recurrent in oxalamates **2** and **3**, and in oxalamide **5**. This motif appears associated with *pd*–π-stacking interactions between the phenyl spacers in oxalamates **2** and **3**, but not in **5**. This motif is also observed in diamides derived from 2,4,6-trimethyl-benzene-1,3-diamine[18] and strongly resembles the supramolecular staircase 1-D motif shown by polymorph **1**.

In spite of the presence of sterically demanding groups in **5** and **6**, the $R_2^2(10)$ (NH···OC) oxalamide supramolecular motif persists, in contrast with CCDB searches which suggest that in most of the cases when this motif was not present this was due to severe derivatization or the presence of sterically demanding groups.[31] The intermolecular spacing along the oxalamide $R_2^2(10)$ tape, in **5** and **6**, is in the reported range for other oxalamides.[7e] Among the set of compounds analyzed, compound **5** shows both $R_2^2(10)$ and $R_2^2(16)$ ring motifs, however this last is not associated with π-stacking interactions, mainly because of the length of the oxalamide arm whose involvement in $R_2^2(10)$ hydrogen bonding motif slips the phenyl planes beyond the limits for such interaction. Whereas the 1-D *meso*-helix arrangement of oxalamide **6** is similar to that reported for polymorph **1′**.

On the other hand, the PhNHCO groups are exclusively engaged in intramolecular three-centred hydrogen bonding, in compounds **4** and **7**, and thus are not available for intermolecular interactions. Extensive intramolecular hydrogen bonding, especially when at least four adjacent rings of six or five members are formed, avoids the participation of the amide group in intermolecular hydrogen bonding as has also been observed for oxalamides derived from amino acids.[7e] Such is the case of compounds **4** and **7**. However, in contrast with similar

bis-aryloxalamides/oxalamates *o*-substituted with groups capable of HB, which are characterized for their lack of a supramolecular structure,[22] compounds **4** and **7** form well defined 2-D crystal networks built by the concurrence of more varied interactions: CO···CO, C–H···A (A=O, π) and π-stacking interactions, additionally strengthened by NH···OH, OH···O=C HB in oxalamide **7**. Among them, CO···CO interactions play an important role since they are comparable with hydrogen bonding.[28]

Blocking 4 and 6 positions is required to maintain a reliable out of-the-plane conformation on the transformation from oxalamates to oxalamides. Nevertheless, the twisted conformation is not enough for intermolecular HB as reported in bis-oxalamides. Neither twisted nor planar conformation forms homomeric intermolecular hydrogen bonding, since bis-oxalamides are discrete units in the solid state.[13] The increase in the number of moieties per molecule capable of forming non-covalent interactions plays a decisive role. Thus in 1,3-phenyl-dioxalamates/dioxalamides both twisted and planar conformations are capable to develop 2-D networks.

4. Conclusions

Conformational control of the oxalamate/oxalamide cavities was demonstrated through the use of substituents in the C-2 position. The bulky methyl group favours the out-of-plane conformation in compounds **2** and **5**. Whereas the participation of the methyl group in C–H···OC interactions favors the *endo* conformation of the phenylamide carbonyl. Further increasing steric strain with methyl groups in C–4 and C–6 permanently fixes the twisted conformation in compounds **3** and **6**. Meanwhile the cooperative participation of the bulky OMe group and its hydrogen-bonding accepting nature leads to the *exo* conformation in compounds **4** and **7**. Particularly the role of intramolecular three-centred hydrogen bonding interactions in the stabilization of the *exo* (*ap*)–*exo*(*ap*) conformation was demonstrated by variable temperature ^{1}H NMR experiments and IR spectra.

Intramolecular hydrogen-bonding interactions are determinant in the adopted conformation and exert a strong influence on the nature of non-covalent interactions that rule the organization at the supramolecular level. More than four adjacent $S(n)$ rings ($n = 5, 6$), in the same molecule, avoid intermolecular hydrogen bonding leading to CO···CO, C–H···A (A=O, π) and π-stacking interactions to direct the crystal organization in compound **4** and **7**, strengthened by NH···OH, OH···O=C hydrogen bonding in this last.

The twisted conformation of the oxalamate moiety, in compounds **2** and **3**, allowed the formation of $R_2^2(16)$ NH···OC motif which appears associated with *pd*–π-stacking interactions between the phenyl spacers. This motif strongly resembles the reported one for polymorph **1**. In contrast, the twisted conformation of the oxalamide moiety, in compound **6**, forms the robust oxalamide tapes characterized by the occurrence of the $R_2^2(10)$ NH···OC motif, developing *meso*-helices in 1-D, in close similarity with the reported structure of polymorph **1'**. Oxalamide **5** shows both $R_2^2(16)$ and $R_2^2(10)$ motifs forming rough 2-D sheets.

Supramolecular versatility of phenyl-oxalamate/oxalamide moieties was demonstrated by means of the formation of dimers

(0-D), π-stacked columns, tapes, chains, or helixes (1-D) and sheets or walls (2-D). The lengthening of the oxalyl arm in oxalamides in comparison with oxalamates, slips the phenyl rings beyond π-stacking interactions, in compound **5**, and enlarges the turn of the helix in compound **6**. Dimensionality is not increased on going from oxalamates **2–4** to oxalamides **5–7**, just the 2-D is strengthened showing more complex networks.

The conformations of amide/oxalamate/oxalamide derivatives of the parent 2,4,6-trimethyl-benzene-1,3-diamine and 5-*tert*-butyl-2,6-diamineanisol are reliable, the former is twisted up and down from the phenyl spacer and the latter is planar and *exo* to the cavity. In contrast, amide/oxalamate/oxalamide derivatives of both 1,3-diaminobenzene and 2-methyl-benzene-1,3-diamine are more versatile, their final conformation will depend on the forces that bind the crystal lattice.

Among the set of studied compounds, oxalamide derivatives of 2,4,6-trimethyl-benzene-1,3-diamine are prone to form 1-D *meso*-helix supramolecular architectures. The turn of the helix could be modulated by the pendant RNHCO residue.

5. Experimental

5.1 General methods

All chemicals and solvents were of reagent grade and used as received. Melting points were measured on an Electrothermal IA 9100 apparatus and were uncorrected. IR spectra were recorded neat using a Varian 3100 FT-IR with ATR system Excalibur Series spectrophotometer. Mass spectra were obtained in a Bruker Esquire 6000 spectrometer with an electron ionization mode. ^{1}H and ^{13}C NMR spectra were recorded on a Varian Mercury 300 (^{1}H, 300.08; ^{13}C, 75.46 MHz) instrument in CDCl$_3$ solutions (**2–4**) or DMSO-d$_6$ (**5–7**), measured with SiMe$_4$ as the internal reference, chemical shifts are in ppm and ^nJ(H–H) in hertz. Variable temperature experiments were performed in the same apparatus equipped with a temperature controller to keep the temperature constant within 0.3 °C, from 20–120 °C in 10 °C increments with a delay of 5 min for temperature stabilization. Each spectrum was recorded with 16 scans.

XRD experiments. Single-crystal X-ray diffraction data for molecules **2–7** were collected on a Bruker Apex II or Nonius Kappa area detector diffractometers at 293(2) K (**2–4**) or 173(2) K (**5–7**) with Mo Kα radiation, λ = 0.71073 Å. A summary of crystal data and collection parameters is listed in Table 5. A semiempirical absorption correction was applied using SADABS[31] and the program SAINT[32] was used for integration of the diffraction profiles. The structures were solved by direct methods using SHELXS97[33] program of WinGX package.[34] The final refinement was performed by full-matrix least-squares methods on F2 with SHELXL97[32] program. H atoms on C, N and O were positioned geometrically and treated as riding atoms, with C–H = 0.93–0.98 Å, and with U_{iso}(H) = 1.2U_{eq}(C). The program Mercury was used for visualization, molecular graphics and analysis of crystal structures,[35] the software used to prepare material for publication was PLATON.[36] Molecule **4** is disordered in both ethyl and *t*-Bu groups. The ethyl group is disordered over two positions (C11A and C11B, C12A and C12B) with refined occupancy factors 0.538(17) and 0.462(17) while

appropriate similarity restraints were applied to the displacement parameters of both components. The *tert*-butyl group exhibits orientational disorder, which was modelled with two positions. The disordered C atoms were presumed to have the same anisotropic displacement parameters. Furthermore, C–C (methyl) distances in the *tert*-butyl group were restrained to be the same for both orientations. The occupancies of the two sites converged at 0.646 (14) and 0.354 (14). Crystals suitable for X-ray analysis were obtained from THF (compounds **3** and **4**), DMSO (compounds **5**, **6** and **7**) or *N,N*-dimethylformamide (compound **2**). Three batches of crystals from compound **5** were independently obtained and analyzed by XRD to give the same space group and thus the same crystalline structure.

Theoretical calculations. Geometry optimization was carried out using the DFT/PBEPBE method with the 6-31+G (3df, 3pd) basis set. All calculations were done using the Gaussian98 program.[37]

5.2 Synthesis of compounds

Compounds **2** and **3** were prepared as reported.[38]

Diethyl *N,N'*-[1,3-(2-methyl)phenyl]dioxalamate 2. White solid, mp: 134–136 °C, IR ν (neat) (cm^{-1}): 3241 (N–H), 1681 (C=O). ^{1}H NMR: 8.86 (s, 2H, NH), 7.70 (d, 2H, $^3J = 8.2$), 7.28 (t, 1H, $^3J = 8.2$), 4.42 (q, 4H, O–CH_2, $^3J = 7.0$), 2.20 (s, 3H, CH_3), 1.42 (t, 6H, CH_2–CH_3, $^3J = 7.0$). ^{13}C NMR: 161.1 (C9), 154.5 (C8), 134.9 (C1, C3), 127.4 (C5), 123.0 (C2), 121.4 (C4, C6), 64.1 (C11), 14.2 (C12), 12.3 (Me). ESI MS [M + Na]$^+$ = 344.8 *m/z*. Anal. Calcd for C$_{15}$H$_{18}$N$_2$O$_6$ (%): C 55.90, H 5.63, N 8.69. Found: C 55.58, H 5.75, N 9.09.

Diethyl *N,N'*-[1,3-(2,4,6-trimethyl)phenyl]dioxalamate 3. White solid, mp: 194–196 °C, IR ν (neat) (cm^{-1}): 3225 (N–H), 1685 (C=O). ^{1}H NMR: 8.47 (s, 2H, NH), 7.00 (s, 1H, Ph), 4.39 (q, 4H, O–CH_2, $^3J = 7.1$), 2.17 (s, 6H, 2CH_3), 2.06 (s, 3H, CH_3), 1.41 (t, 6H, CH_2–CH_3, $^3J = 7.1$). ^{13}C NMR: 160.9 (C9), 155.1 (C8), 135.3

(C1, C3), 132.7 (C4, C6), 130.8 (C5), 130.4 (C2), 63.9 (C11), 18.5 (2Me), 14.3 (Me), 14.1 (C12). ESI MS [M + Na]$^+$ = 372.8 *m/z*. Anal. Calcd for C$_{17}$H$_{22}$N$_2$O$_6$ (%): C 58.28, H 6.33, N 8.00. Found C 58.03, H 6.25, N 10.56.

Diethyl *N,N'*-[1,3-(5-*tert*-butyl-2-methoxy)phenyl]-dioxalamate 4. 5-*tert*-Butyl-2,6-diamineanisol (2 g, 10.2 mmol) in THF (50 ml) and triethylamine (3.15 ml, 22.61 mmol) was treated dropwise under vigorous stirring with ethyl chlorooxalacetate (2.52 ml, 22.61 mmol) at 5–10 °C. After stirring for an additional 24 h at 25 °C, the solid was removed and washed with THF to give **4** (12.43 g, 87.2% yield) as a yellow solid, mp: 173–175 °C. IR ν (neat) (cm^{-1}): 3372 (N–H), 1708 (C=O). ^{1}H NMR: 9.25 (s, 2H, NH), 8.21 (s, 2H, Ph), 4.40 (q, 4H, O–CH_2, $^3J = 7.1$), 3.81 (s, 3H, O–CH_3), 1.38 (t, 6H, –CH_2–CH_3, $^3J = 7.1$), 1.28 (s, 9H, 3CH_3). ^{13}C NMR: 160.8 (C9), 154.1 (C8), 149.2 (C2), 137.0 (C5), 129.4 (C1, C3), 114.7 (C4, C6), 63.9 (C11), 61.7 (MeO), 35.3 (C(Me)$_3$), 31.3 (3Me), 14.3 (C12). ESI MS [M + Na]$^+$ = 416.9 *m/z*. Anal. Calcd for C$_{19}$H$_{26}$N$_2$O$_7$ (%): C 57.86, H 6.64, N 7.10. Found (%): C 57.80, H 6.60, N 7.44.

N^1,$N^{1'}$-(1,3-(2-Methyl)-phenyl)-bis-(N^2-(2-hydroxyethyl)-oxalamide) 5. A solution of **2** (0.3 g, 0.930 mmol) in methanol (30 ml) and ethanolamine (0.111 ml, 1.861 mmol) was refluxed for 24 h. The suspension was filtered off and the resulting solid was washed with acetone (3 ml) and dried to yield 0.327 g (50.6%) of a white solid, mp: 232–234 °C. IR ν (neat) (cm^{-1}): 3282 (N–H), 1657 (C=O) cm^{-1}. ^{1}H NMR: 10.28 (s, 2H, N7–H), 8.78 (t, 2H, N10–H), 7.18–7.29 (m, 3H, Ph), 4.70 (b, 2H, OH), 3.48 (t, 4H, OCH$_2$), 3.26 (q, 4H, NCH$_2$), 2.01 (s, 3H, Ar–CH_3). ^{13}C NMR: 160.2 (C9), 159.4 (C8), 136.4 (C1), 129.2 (C5), 126.3 (C2), 124.3 (C4), 59.8 (C12), 42.5 (C11), 13.4 (Me). ESI MS [M + Na]$^+$ = 374.8 *m/z*. Anal. Calcd for C$_{15}$H$_{20}$N$_4$O$_6$ (%): C 51.13, H 5.72, N 15.90. Found (%): C 51.03, H 6.00, N 15.90.

N^1,$N^{1'}$-(1,3-(2,4,6-Trimethyl)-phenyl)-bis-(N^2-(2-(2-hydroxy-ethoxy)ethyl)oxalamide) 6. A solution of **3** (0.5 g, 1.427 mmol) in methanol (30 ml) and 2-(2-aminoethoxy)-ethanol (0.284 ml,

Table 5 Crystal data and collection parameters

Parameter	Compound					
	2	**3**	**4**	**5**	**6**	**7**
CCDC no.	795133	801211/795129	795131	801212	801213	801214
Formulae	C$_{15}$H$_{18}$N$_2$O$_6$	C$_{17}$H$_{22}$N$_2$O$_6$	C$_{19}$H$_{26}$N$_2$O$_7$	C$_{15}$H$_{20}$N$_4$O$_6$	C$_{21}$H$_{32}$N$_4$O$_8$	C$_{19}$H$_{28}$N$_4$O$_7$
Form. Wt.	322.31	350.37	394.42	352.35	468.5	424.5
Crystal system	Monoclinic	Monoclinic	Triclinic	Triclinic	Monoclinic	Monoclinic
Space group	$P2_1/c$	$P2_1/c$	$P\bar{1}$	$P\bar{1}$	$C2/c$	$C2/c$
a/Å	8.2302(12)	8.0352(7)	9.9640(3)	9.0080(18)	11.4567(6)	13.0660(30)
b/Å	23.218(3)	16.0173(14)	10.2180(3)	9.5510(19)	12.9050(7)	24.3840(50)
c/Å	8.1795(12)	14.3980(14)	10.5790(4)	10.5930(19)	16.4558(10)	13.3030(30)
α/°	90	90	80.969(2)	94.800(20)	90.000(0)	90.000(0)
β/°	94.665(2)	102.681(2)	87.691(2)	99.010(30)	101.828(2)	90.000(30)
γ/°	90	90	87.649(2)	109.340(30)	90.000(0)	90.000(0)
V/Å^3	1557.8(4)	1807.9(3)	1062.20	840.3(3)	2381.31(10)	4238.35(16)
Z	4	4	2	2	4	8
Measured reflections	14 126	10 973	11 563	5214	7143	11 757
Independent reflections	2745	3184	3246	2956	2096	3613
GOOF	1.160	1.050	1.157	0.960	0.820	1.121
R_{int}	0.030	0.060	0.125	0.033	0.050	0.071
$R[F^2 > 2\sigma(F^2)]$	0.054	0.052	0.082	0.080	0.068	0.055
w$R(F^2)$	0.125	0.103	0.215	0.243	0.170	0.186

2.854 mmol) was refluxed for 24 h. The suspension was filtered off and the resulting solid was washed with acetone (3 ml) and dried to yield 0.462 g (70.29%) of a white solid, mp: 192–194 °C. IR ν (neat) (cm^{-1}): 3299 (N–H), 1663 (C=O). ^{1}H NMR: 10.20 (s, broad 2H, N7–H), 8.73 (t, 2H, N10–H), 7.00 (s, 1H, Ph), 4.20 (broad, 2H, OH), 3.53 (m, 4H, CH$_2$OH), 3.48 (m, 4H, CH$_2$O–CH$_2$), 3.46 (m, 4H, CH$_2$–OCH$_2$), 3.36 (m, 4H, NCH$_2$), 2.09 (s, 6H, 2CH$_3$), 1.91 (s, 3H, CH$_3$). ^{13}C NMR (δ ppm DMSO-d$_6$): 160.6 (C9), 159.5 (C8), 134.5 (C4), 133.4 (C1), 132.9 (C5), 129.4 (C2), 72.7 (C12), 68.9 (C15), 60.8 (C14), 39.7 (C11), 18.5 (2Me), 14.1 (Me). Anal. Calcd for C$_{22}$H$_{34}$N$_4$O$_7$ (%): C 53.84, H 6.88, N 11.96. Found (%): C 53.60, H 7.20, N 11.19.

N^1,$N^{1'}$-(1,3-(5-*tert*-Butyl-2-methoxy)-phenyl)-bis-(N^2-(2-hydroxy-ethyl)oxalamide) 7. A solution of **4** (0.4 g 1.01 mmol) in ethanol (30 ml) and ethanolamine (0.122 ml, 2.02 mmol) was refluxed for 24 h. The solution was evaporated and the resulting solid was washed with cold ethanol (3 ml) and dried to yield 0.205 g (47.7%) of a white solid, mp: 234–237°C. IR ν (neat) (cm^{-1}): 3351 (N–H), 1667 (C=O). ^{1}H NMR: 9.86 (s, 2H, N7–H), 8.91 (t, 2H, N10–H), 7.88 (s, 2H, Ph), 4.83 (t, 2H, OH), 3.76 (s, 3H O–CH$_3$), 3.50 (t, 4H, OCH$_2$), 3.25 (q, 4H, NCH$_2$), 1.24 (s, 9H, 3CH$_3$). ^{13}C NMR: 160.3 (C9), 158.6 (C8), 147.5 (C2), 140.3 (C5), 130.0 (C1, C3), 116.1 (C4, C6), 59.7 (3CH$_3$), 61.7 (O–Me), 42.7 (C–(CH$_3$)$_3$). Anal. Calcd for C$_{19}$H$_{28}$N$_4$O$_7$ (%): C 53.76, H 6.65, N 13.20. Found (%): C 53.73, H 6.71, N 12.78.

Acknowledgements

References

1 J. W. Steed and J. L. Atwood, *Supramolecular Chemistry*, John Wiley & Sons, Ltd., UK, 2nd edn, 2009.
2 (*a*) T. Shimizu, M. Masuda and H. Minamikawa, *Chem. Rev.*, 2005, **105**, 1401; (*b*) E. R. Kay, D. A. Leigh and F. Zerbetto, *Angew. Chem., Int. Ed.*, 2007, **46**, 72; (*c*) J. D. Fox and S. J. Rowan, *Macromolecules*, 2009, **42**, 6823–6835.
3 E. T. Kool, *Chem. Rev.*, 1997, **97**, 1473.
4 T. Bugg, *Introduction to Enzyme and Coenzyme Chemistry*, Blackwell Publishing Ltd, Oxford, UK, 2004.
5 O. Keskin, A. Gursoy, B. Ma and R. Nussinov, *Chem. Rev.*, 2008, **108**, 1225.
6 S. D. Sarker and L. Nahar, *Chemistry for Pharmacy Students: General, Organic and Natural Product Chemistry*, John Wiley & Sons Ltd, London, England, 2007.
7 (*a*) P. W. Baures, J. R. Rush, A. V. Wiznycia, J. Desper, B. A. Helfrich and A. M. Beatty, *Cryst. Growth Des.*, 2002, **6**, 653; (*b*) O. Ugono, N. P. Rath and A. M. Beatty, *Cryst. Growth Des.*, 2009, **9**, 4595; (*c*) C. B. Aakeroy, J. Desper and J. F. Urbina, *Chem. Commun.*, 2005, 2820; (*d*) C. B. Aakeroy, J. Desper and I. Hussain, *Cryst. Growth Des.*, 2006, **6**, 474; (*e*) T. L. Nguyen, F. W. Fowler and J. W. Lauher, *J. Am. Chem. Soc.*, 2001, **123**, 11057.
8 J. W. Lauher, *ACA Trans.*, 2004, **39**, 31.
9 (*a*) R. Marx, S. J. Glasera and M. Bolte, *Acta Crystallogr., Sect. E: Struct. Rep. Online*, 2003, **59**, o1425; (*b*) F. J. Martínez-Martínez, P. Maya-Lugardo, E. V. García-Báez, H. Höpfl, J. Hernández-Díaz and I. I. Padilla-Martínez, *Acta Crystallogr., Sect. E: Struct. Rep. Online*, 2005, **61**, o2994; (*c*) S. Coe, J. J. Kane, T. L. Nguyen, L. M. Toledo, E. Wininger, F. W. Fowler and J. W. Lauher, *J. Am. Chem. Soc.*, 1997, **119**, 86; (*d*) T. L. Nguyen, A. Scott,

10 B. Dinkelmeyer, F. W. Fowler and J. W. Lauher, *New J. Chem.*, 1998, 129.
10 (*a*) M. C. Muñoz, G. Blay, I. Fernández, J. R. Pedro, R. Carrasco, M. Castellano, R. Ruiz-García and J. Cano, *CrystEngComm*, 2010, **12**, 2473; (*b*) I. I. Padilla-Martínez, M. Chaparro-Huerta, F. J. Martínez-Martínez, H. Höpfl and V. García-Báez, *Acta Crystallogr., Sect. E: Struct. Rep. Online*, 2003, **59**, o825; (*c*) G. Blay, I. Fernandez, J. R. Pedro, R. Ruiz-García, M. C. Muñoz, J. Cano and R. Carrasco, *Eur. J. Org. Chem.*, 2003, 1627; (*d*) G. Francese, A. Neels, H. Stoeckli-Evans and S. Decurtins, *Acta Crystallogr., Sect. C: Cryst. Struct. Commun.*, 1998, **54**, o1858.
11 A. D. McNaught and A. Wilkinson, *IUPAC. Compendium of Chemical Terminology (the "Gold Book")*, Blackwell Scientific Publications, Oxford, UK, 2nd edn, 1997.
12 J. Bernstein, R. E. Davis, L. Shimoni and N.-L. Chang, *Angew. Chem.,Int. Ed. Engl.*, 1995, **34**, 1555.
13 B. Piotrkowska, M. Gdaniec, M. J. Milewska and T. Połonski, *CrystEngComm*, 2007, **9**, 868.
14 E. V. Garcia-Baez, C. Z. Gomez-Castro, H. Hopfl, F. J. Martinez-Martinez and I. I. Padilla-Martinez, *Acta Crystallogr., Sect. C: Cryst. Struct. Commun.*, 2003, **59**, o541.
15 G. Pickaert, M. Cesario and R. Ziessel, *J. Org. Chem.*, 2004, **69**, 5335.
16 (*a*) P. Gilli, V. Bertolasi, V. Ferretti and G. Gilli, *J. Am. Chem. Soc.*, 2000, **122**, 10405; (*b*) A. Saeed, S. Hussain and M. Bolte, *Acta Crystallogr., Sect. E: Struct. Rep. Online*, 2008, **64**, o521; (*c*) C. P. Price, A. L. Grzesiak, J. W. Kampf and A. J. Matzger, *Cryst. Growth Des.*, 2003, **3**, 1021.
17 A. Bondi, *J. Phys. Chem.*, 1964, **68**, 441.
18 H. Allouchi, M. Cotrait and J. Malthête, *Mol. Cryst. Liq. Cryst.*, 2001, **362**, 101.
19 Y.-Y. Zhu, J. Wu, C. Li, J. Zhu, J.-L. Hou, C.-Z. Li, X.-K. Jiang and Z.-T. Li, *Cryst. Growth Des.*, 2007, **7**, 1490.
20 (*a*) R. Wieczorek and J. J. Dannenberg, *J. Am. Chem. Soc.*, 2003, **125**, 14065; (*b*) R. Viswanathan, A. Asensio and J. J. Dannenberg, *J. Phys. Chem. A*, 2004, **108**, 9205.
21 R. Taylor, O. Kennard and W. Versichel, *J. Am. Chem. Soc.*, 1984, **106**, 244.
22 F. J. Martínez-Martínez, I. I. Padilla-Martínez, M. A. Brito, E. D. Geniz, R. C. Rojas, J. B. R. Saavedra, H. Höpfl, M. Tlahuextl and R. Contreras, *J. Chem. Soc., Perkin Trans. 2*, 1998, 401.
23 I. I. Padilla-Martínez, F. J. Martínez-Martínez, C. I. Guillén-Hernández, M. Chaparro-Huerta, L. C. Cabrera-Pérez, C. Z. Gómez-Castro, B. A. López-Romero and E. V. García-Báez, *ARKIVOC*, 2005, 401.
24 H. O. Desseyn, S. P. Perlepes, K. Clou, N. Blaton, B. J. V. d. Veken, R. Dommisse and P. E. Hansen, *J. Phys. Chem. A*, 2004, **108**, 5175.
25 I. I. Padilla-Martínez, F. J. Martínez-Martínez, E. V. García-Báez, J. M. Torres-Valencia, S. Rojas-Lima and H. Höpfl, *J. Chem. Soc., Perkin Trans. 2*, 2001, 1817.
26 T. Steiner, *Angew. Chem., Int. Ed.*, 2002, **41**, 48.
27 G. R. Desiraju, *Acc. Chem. Res.*, 1996, **29**, 441.
28 M. Nishio, *CrystEngComm*, 2004, **6**, 130.
29 F. H. Allen, C. A. Baalham, J. P. M. Lommerse and P. R. Raithby, *Acta Crystallogr., Sect. B: Struct. Sci.*, 1998, **54**, 320.
30 (*a*) J. H. Williams, *Acc. Chem. Res.*, 1993, **26**, 593; (*b*) I. Dance and M. Scudder, *Chem.–Eur. J.*, 1996, **2**, 481.
31 M. Hoffman, U. Rychlewska and B. Warżajtis, *CrystEngComm*, 2005, **7**, 260.
32 Bruker, *APEX II, SAINT, SADABS and SHELXTL*, Bruker AXS Inc., Madison, Winsconsin, USA, 2004.
33 G. M. Sheldrick, *Acta Crystallogr., Sect. A: Found. Crystallogr.*, 2008, **64**, 112.
34 L. J. Farrugia, *J. Appl. Crystallogr.*, 1999, **32**, 837.
35 C. F. Macrae, P. R. Edgington, P. McCabe, E. Pidcock, G. P. Shields, R. Taylor, M. Towler and J. van de Streek, *J. Appl. Crystallogr.*, 2006, **39**, 453.
36 A. L. Spek, *J. Appl. Crystallogr.*, 2003, **36**, 7.
37 M. J. Frisch, G. W. Trucks, H. B. Schlegel, G. E. Scuseria, M. A. Robb, J. R. Cheeseman, V. G. Zakrzewski, J. A. Montgomery, Jr, J. C. Burant, S. Dapprich, J. M. Millam, A. D. Daniels, K. N. Kudin, M. C. Strain, O. Farkas, J. Tomasi, V. Barone, M. Cossi, R. Cammi, B. Mennucci, C. Pomelli, C. Adamo, S. Clifford, J. Ochterski, G. A. Peterson, P. Y. Ayala, Q. Cui, K. Morokuma, D. K. Malick,

A. D. Rabuck, K. Raghavachari, J. B. Foresman, J. Cioslowski, J. V. Ortiz, A. G. Baboul, B. B. Stefanov, G. Liu, A. Liashenko, P. Piskorz, I. Komaromi, R. Gomperts, R. L. Martin, D. J. Fox, T. Keith, M. A. Al-Laham, C. Y. Peng, A. Nanayakkara, M. Challacombe, P. M. W. Gill, B. Johnson, W. Chen, M. W. Wong, J. L. Andres, C. Gonzalez, M. Head-Gordon, E. S. Replogle and J. A. Pople, *Gaussian 98, Revision A.9*, Gaussian, Inc., Pittsburgh, PA 1998.

38 (*a*) J. B. Wright, C. M. Hall and H. G. Johnson, *J. Med. Chem.*, 1978, **21**, 930; (*b*) E. Pardo, R. Ruiz-García, F. Lloret, M. Julve, J. Cano, J. Pasan, C. Ruiz-Perez, Y. Filali, L.-M. Chamoreau and Y. Journaux, *Inorg. Chem.*, 2007, **46**, 4504.